
Systematic Nuclear Uncertainties in the Hypertriton System

Thiri Yadanar Htun · Daniel Gazda ·
Christian Forssén · Yupeng Yan

Received: date / Accepted: date

Abstract The hypertriton bound state is relevant for inference of knowledge about the hyperon–nucleon (YN) interaction. In this work we compute the binding energy of the hypertriton using the *ab initio* hypernuclear no-core shell model (NCSM) with realistic interactions derived from chiral effective field theory. In particular, we employ a large family of nucleon–nucleon interactions with the aim to quantify the theoretical precision of predicted hypernuclear observables arising from nuclear-physics uncertainties. The three-body calculations are performed in a relative Jacobi-coordinate harmonic oscillator basis and we implement infrared correction formulas to extrapolate the NCSM results to infinite model space. We find that the spread of the predicted hypertriton binding energy, attributed to the nuclear-interaction model uncertainty, is about 100 keV. In conclusion, the sensitivity of the hypertriton binding energy to nuclear-physics uncertainties is of the same order of magnitude as experimental uncertainties such that this bound-state observable can be used in the calibration procedure to constrain the YN interactions.

Keywords Hypernuclei · Ab initio calculations · No-core shell model · Model uncertainties

1 Introduction

Hypernuclei play an essential role in understanding the interactions between nucleons and hyperons. Unlike the case of nuclear interactions—with a vast database of precisely measured low-energy nucleon–nucleon (NN) observables—the available experimental data on (YN) scattering are much poorer both in quantity and quality.

Fortunately, there is an immense amount of information on YN interactions encoded in precision measurements of hypernuclear properties, such as the A hyperon separation energies and excitation spectra, which has been collected over the past decades [1]. However, the utilisation of precise experimental data on hypernuclear spectroscopy to constrain the underlying YN interactions is a very challenging task. First, the computationally-demanding *ab initio* methods, which do not rely on uncontrolled approximations to renormalize the hypernuclear interactions, started to emerge only recently [2, 3, 4, 5, 6, 7, 8]. Second, it is very important to understand all sources of uncertainties in the calculations to quantify the theoretical precision of relevant observables. The main source of uncertainty in *ab initio* calculations of light hypernuclei is the hypernuclear Hamiltonian, constructed from particular models of nuclear and hypernuclear interactions. Besides the poorly constrained YN interactions, the remaining freedom in the construction of realistic nuclear forces represents an additional source of model uncertainty which propagates into hypernuclear observables. In recent years, there has been significant progress in the uncertainty quantification

T.Y. Htun^{1,2,4} · D. Gazda^{1,3} · C. Forssén¹ · Y. Yan²

¹Department of Physics, Chalmers University of Technology, SE-412 96 Göteborg, Sweden

²School of Physics and Center of Excellence in High Energy Physics and Astrophysics, Suranaree University of Technology, Nakhon Ratchasima, 30000, Thailand

³Nuclear Physics Institute of the Czech Academy of Sciences, 25068 Řež, Czech Republic

⁴Department of Physics, University of Mandalay, 05032 Mandalay, Myanmar

in nuclear forces [9, 10, 11, 12, 13], which allowed to provide theoretical uncertainties in nuclear structure calculations [11, 13, 14, 15].

In this work, we study the sensitivity of the hypertriton binding energy to systematic model uncertainties in the nuclear interactions. This information is very important for the future use of this observable to constrain the YN interactions. More specifically we perform hypernuclear NCSM calculations in relative Jacobi-coordinate harmonic oscillator (HO) basis with a family of 42 realistic chiral NN interactions (introduced in Sec. 2.3) while keeping the YN interaction fixed. We study in detail the convergence properties of the NCSM calculations and the dependence of observables on the NCSM model-space parameters. Moreover, we apply infrared (IR) correction formulas [16] to extrapolate the results obtained in finite model spaces to infinite model space, in the hypernuclear NCSM. We present results for the hypertriton ground-state energy and discuss the consequences of our findings. In general, this study serves as a starting point for the uncertainty quantification of other hypernuclear observables.

2 Methodology

2.1 Three-body system in the hypernuclear no-core shell model

The starting point to study the hypertriton within the hypernuclear NCSM approach [5] is the nonrelativistic Hamiltonian for three particles interacting by realistic YN and NN interactions

$$H = - \sum_{i=1}^3 \frac{\hbar^2}{2m_i} \vec{\nabla}_i^2 + V_{NN}(\vec{r}_1, \vec{r}_2) + \sum_{i=1}^2 V_{YN}(\vec{r}_i, \vec{r}_3) + \Delta M, \quad (1)$$

where the coordinates \vec{r}_i and masses m_i correspond to nucleons for $i = 1, 2$ and for $i = 3$ to a hyperon. Since we explicitly take into account the strong-interaction $\Lambda N \leftrightarrow \Sigma N$ transitions in V_{YN} [17], the Λ -hypernuclear states are coupled with Σ -hypernuclear states. To account for the mass difference of these states, the mass term ΔM is introduced in Eq. (1).

The formulation of NCSM which is particularly suitable for few-body hypernuclear systems employs a translationally-invariant HO basis defined in relative Jacobi coordinates and the associated momenta. For an $A = 3$ hypernucleus we need to introduce two different sets of Jacobi coordinates. The first set, expressed in term of rescaled single-particle coordinates $\vec{x}_i = \sqrt{m_i} \vec{r}_i$, is defined as

$$\begin{aligned} \vec{\xi}_0 &= \frac{1}{\sum_{i=1}^3 m_i} \sum_{i=1}^3 \sqrt{m_i} \vec{x}_i, \\ \vec{\xi}_1 &= \sqrt{\frac{1}{2}} (\vec{x}_1 - \vec{x}_2), \\ \vec{\xi}_2 &= \sqrt{\frac{2m_N m_Y}{2m_N + m_Y}} \left[\frac{1}{2\sqrt{m_N}} (\vec{x}_1 + \vec{x}_2) - \frac{1}{\sqrt{m_Y}} \vec{x}_3 \right], \end{aligned} \quad (2)$$

where m_N and m_Y are the nucleon and hyperon (Λ or Σ) masses. In this set, the coordinate $\vec{\xi}_0$ is proportional to the center of mass (c.m.) coordinate of the $A = 3$ system, $\vec{\xi}_1$ is proportional to the relative coordinate of the nucleons, and $\vec{\xi}_2$ is proportional to the relative coordinate of the hyperon with respect to the c.m. coordinate of the nucleon pair. Since the interaction terms in the Hamiltonian (1) depend only on the relative coordinates, the center of mass motion, associated with $\vec{\xi}_0$, can be eliminated to decrease the dimensionality of the problem. Consequently, the intrinsic wave function of the $A = 3$ system can be expanded in a complete set of HO basis states

$$|(n_{NN}(l_{NN}s_{NN})j_{NN}t_{NN}, \mathcal{N}_Y \mathcal{L}_Y \mathcal{J}_Y \mathcal{T}_Y)JT\rangle \quad (3)$$

characterized by a single HO frequency $\hbar\omega$, where $|n_{NN}(l_{NN}s_{NN})j_{NN}t_{NN}\rangle$ and $|\mathcal{N}_Y \mathcal{L}_Y \mathcal{J}_Y \mathcal{T}_Y\rangle$ are HO states, depending on the coordinates $\vec{\xi}_1$ and $\vec{\xi}_2$, respectively. The $n_{NN}(\mathcal{N}_Y)$, $l_{NN}(\mathcal{L}_Y)$, $s_{NN}(\frac{1}{2})$, $j_{NN}(\mathcal{J}_Y)$, $t_{NN}(\mathcal{T}_Y)$ are the radial, orbital, spin, angular momentum, and isospin quantum numbers corresponding to the relative two-nucleon (hyperon) state. The NN and hyperon ($Y = \Lambda, \Sigma$) states are coupled to the total

angular momentum J and isospin T . Antisymmetry of the states (3) with respect to nucleon interchange is achieved by restricting the two-nucleon channel quantum numbers by the condition $(-1)^{l_{NN}+s_{NN}+t_{NN}} = -1$. The set of Jacobi coordinates (2) is convenient for the construction of antisymmetric translationally-invariant HO basis and evaluation of the NN interaction matrix elements. It is not, however, suitable for the evaluation of the YN interaction matrix elements.

In order to evaluate the V_{YN} matrix elements, another set of Jacobi coordinates is needed. The new set is obtained from the set (2) by keeping the coordinate $\vec{\xi}_0$ and introducing two new coordinates

$$\begin{aligned}\vec{\eta}_1 &= \sqrt{\frac{(m_N + m_Y)m_N}{2m_N + m_Y}} \left[\frac{1}{\sqrt{m_N}} \vec{x}_1 - \frac{1}{(m_N + m_Y)} (\sqrt{m_N} \vec{x}_2 + \sqrt{m_Y} \vec{x}_3) \right], \\ \vec{\eta}_2 &= \sqrt{\frac{m_N m_Y}{m_N + m_Y}} \left(\frac{1}{\sqrt{m_N}} \vec{x}_2 - \frac{1}{\sqrt{m_Y}} \vec{x}_3 \right),\end{aligned}\quad (4)$$

where $\vec{\eta}_1$ is the relative coordinate of a nucleon with respect to the c.m. of the YN pair and $\vec{\eta}_2$ is the relative coordinate of the YN pair. The Jacobi coordinates in this set can be obtained by an orthonormal transformation of the coordinates (2). Consequently, the HO states (3) can be expanded as

$$\begin{aligned}|(n_{NN}(l_{NN}s_{NN})j_{NN}t_{NN}, \mathcal{N}_Y \mathcal{L}_Y \mathcal{J}_Y \mathcal{T}_Y)JT\rangle &= \sum_{LS} \widehat{L}^2 \widehat{S}^2 \widehat{j}_{NY} \widehat{\mathcal{J}}_N \widehat{j}_{NN} \widehat{\mathcal{J}}_Y \widehat{s}_{NN} \widehat{s}_{NY} \\ &\times (-1)^{s_{NY}+1/2+s_{NN}+1/2} \begin{Bmatrix} l_{NY} & s_{NY} & j_{NY} \\ \mathcal{L}_N & 1/2 & \mathcal{J}_N \\ L & S & J \end{Bmatrix} \begin{Bmatrix} l_{NN} & s_{NN} & j_{NN} \\ \mathcal{L}_Y & 1/2 & \mathcal{J}_Y \\ L & S & J \end{Bmatrix} \begin{Bmatrix} 1/2 & 1/2 & s_{NN} \\ 1/2 & S & s_{NY} \end{Bmatrix} \\ &\times (-1)^{t_{NY}+\mathcal{T}_N+t_{NN}+\mathcal{T}_Y} \widehat{t}_{NY} \widehat{t}_{NN} \begin{Bmatrix} 1/2 & 1/2 & t_{NN} \\ t_Y & T & t_{NY} \end{Bmatrix} (-1)^{\mathcal{L}_N+\mathcal{L}_Y} \\ &\times \langle n_{NY} l_{NY} \mathcal{N}_N \mathcal{L}_N | n_{NN} l_{NN} \mathcal{N}_Y \mathcal{L}_Y \rangle_{\frac{2m_N+m_Y}{m_Y}} |(n_{NY}(l_{NY}s_{NY})j_{NY}t_{NY}, \mathcal{N}_N \mathcal{L}_N \mathcal{J}_N)JT\rangle\end{aligned}\quad (5)$$

in terms of HO basis states

$$|(n_{NY}(l_{NY}s_{NY})j_{NY}t_{NY}, \mathcal{N}_N \mathcal{L}_N \mathcal{J}_N)JT\rangle, \quad (6)$$

where $|n_{NY}(l_{NY}s_{NY})j_{NY}t_{NY}\rangle$ and $|\mathcal{N}_N \mathcal{L}_N \mathcal{J}_N\rangle$ are HO states corresponding to the nucleon–hyperon pair and a nucleon and depending on the coordinates $\vec{\eta}_2$ and $\vec{\eta}_1$, respectively. In Eq. (5), $\widehat{j} = \sqrt{2j+1}$, the terms in curly brackets are Wigner 6- and 9- j symbols, and $\langle \cdot | \cdot \rangle_d$ is the general HO bracket for two particles with mass ratio $d = \frac{2m_N+m_Y}{m_Y}$ [18], which facilitates the transformation between coordinates $\vec{\xi}_1, \vec{\xi}_2$ and $\vec{\eta}_2, \vec{\eta}_1$. With the help of expansion (5), it is straightforward to evaluate the V_{YN} matrix elements as

$$\left\langle \sum_{i=1}^2 V_{YN}(\vec{r}_i, \vec{r}_3) \right\rangle = 2 \langle V_{YN}(\vec{\eta}_2) \rangle, \quad (7)$$

where the matrix element on the right hand side is diagonal in all quantum numbers of the states (6), except for n_{NY} and l_{NY} .

NCSM calculations are performed in finite model spaces by diagonalization of the matrix representation of the Hamiltonian (1). The model space is truncated by restricting the maximum number of HO quanta in the basis states (3) as

$$2n_{NN} + l_{NN} + 2\mathcal{N}_Y + \mathcal{L}_Y \leq N_{\max}. \quad (8)$$

The NCSM calculations are thus variational and converge to exact results for $N_{\max} \rightarrow \infty$.

In this work, we employed the leading-order (LO) Bonn–Jülich SU(3)-based χ EFT YN model [17] with regulator cutoff momentum $\Lambda_{YN} = 600$ MeV, together with the NNLO_{sim} family of chiral nuclear interactions at next-to-next-to-leading-order (NNLO) (for details see Sec. 2.3). No renormalization was applied to either of the interactions.

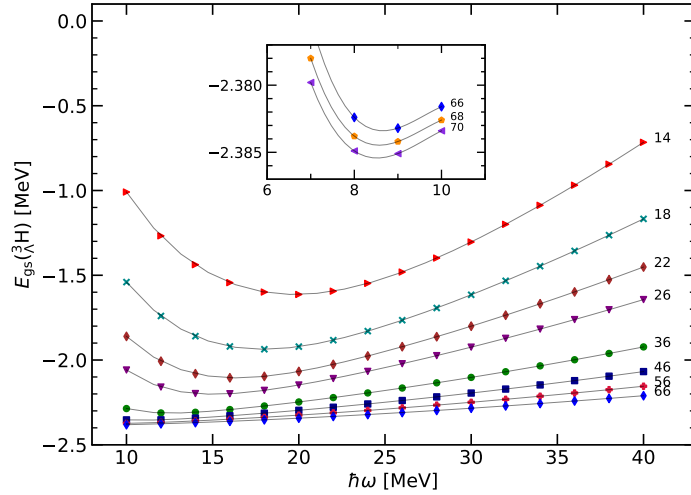


Fig. 1: The ${}^3_{\Lambda}\text{H}$ g.s. energy $E({}^3_{\Lambda}\text{H})$ as a function of the HO frequency $\hbar\omega$, calculated using the NNLO_{sim} Hamiltonian with $\Lambda_{NN} = 500$ MeV and $T_{\text{Lab}}^{\text{max}} = 290$ MeV for several model-space truncations from $N_{\text{max}} = 14$ to $N_{\text{max}} = 70$.

2.2 Infrared Length Scale of the NCSM basis and Extrapolations

IR extrapolation can be used to estimate the infinite-space limit from results computed in truncated model spaces [19,20]. The truncation of the HO basis in terms of model space (N_{max}) and frequency ($\hbar\omega$) can be translated into associated IR and ultraviolet (UV) scales. In particular, for the NCSM basis that is associated with a total energy truncation the corresponding IR scale, L_{eff} , can be extracted by studying the discrete kinetic energy spectrum [16]. The LO IR extrapolation formula for energies is [19]

$$E(L_{\text{eff}}) = E_{\infty} + a_0 e^{-2k_{\infty} L_{\text{eff}}}, \quad (9)$$

where E_{∞} , a_0 and k_{∞} are the fit parameters. Subleading IR corrections have the expected magnitude [21]

$$\sigma_{\text{IR}} \propto \frac{e^{-2k_{\infty} L_{\text{eff}}}}{k_{\infty} L_{\text{eff}}}. \quad (10)$$

In addition, UV corrections to finite-space results can be significant unless $\Lambda_{\text{UV}} \gg \Lambda_{NN}, \Lambda_{YN}$. The IR extrapolation formula (9) is still valid at a fixed UV scale [21]. Such data can be obtained by performing computations at appropriate $(N_{\text{max}}, \hbar\omega)$ model-space parameters. The extrapolated result will then depend on the selected UV scale. This UV dependence can be monitored such that a sufficiently large scale is used to achieve UV-convergence. In this work we find that $\Lambda_{\text{UV}} = 1200$ MeV is sufficient. A more detailed study of IR-, UV-scales and the performance of extrapolation methods in hypernuclear many-body systems will be the topic of future work. In this study we have specifically used IR extrapolation as an independent check of the convergence of the variational minimum.

2.3 Systematic Uncertainties of Nuclear Interactions

The chiral NN interaction model is associated with systematic uncertainties that originate in the selection of calibration data, the truncation of the chiral expansion and possible regulator artefacts. Here we quantify the magnitude of these systematic uncertainties by employing the full family of 42 different interactions at NNLO (labeled NNLO_{sim}) that was constructed by Carlsson et al. [11]. These interactions were obtained using six different truncations of the NN scattering calibration data ($T_{\text{lab}} \leq T_{\text{Lab}}^{\text{max}}$ with

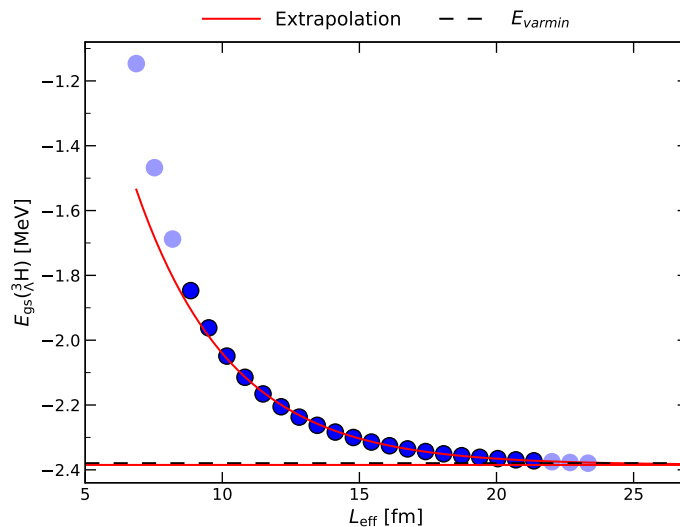


Fig. 2: Extrapolation of $E(\Lambda^3\text{H})$ calculated using the NNLO_{sim} Hamiltonian with $\Lambda_{NN} = 500$ MeV and $T_{\text{Lab}}^{\text{max}} = 290$ MeV for a fixed value of the HO basis UV cutoff $\Lambda_{\text{UV}} = 1200$ MeV. The fit is performed with data $N_{\text{max}} \in [22, 60]$ and compared with the variational minimum at $N_{\text{max}} = 66$.

$T_{\text{Lab}}^{\text{max}} \in [125, 290]$ MeV) and seven different regulator cutoffs ($\Lambda_{NN} \in \{450, 475, \dots, 575, 600\}$ MeV). For each different interaction model, all 26 low-energy constants (LECs) up to NNLO were simultaneously optimised to NN and πN scattering data plus bound-state observables in the few-nucleon sector. The statistical uncertainties in the LECs from the fit have a small effect on the computed hypernuclear binding energies. Instead, we focus our attention on the spread of the predicted hypertriton binding energy obtained with the 42 different interactions. It should be stressed that all these interaction models give an equally good description of the fit data.

3 Results and Discussion

NCSM calculations are performed for the hypertriton with model space truncations $N_{\text{max}} \leq 66$, and in the range of HO frequencies $7 \leq \hbar\omega \leq 40$ MeV with the chiral NNLO_{sim} family of NN interactions and a fixed LO YN interaction. These are basically 42 independent calculations. The hypertriton ground-state energy as a function of the model space truncation and HO frequency $\hbar\omega$ is presented in Fig. 1 for one of the 42 NNLO_{sim} Hamiltonians ($\Lambda_{NN} = 500$ MeV, $T_{\text{Lab}}^{\text{max}} = 290$ MeV). The energy is clearly converging with increasing model space. The slow convergence at large frequencies can be attributed to the small binding energy and long tail of the wave function. Consequently we also computed the energies at $\hbar\omega = 7, 8, 9$ MeV to locate the variational minimum E_{varmin} . The lowest energy for this particular interaction, $E(\Lambda^3\text{H}) = -2.385$ MeV, was found at $\hbar\omega = 9$ MeV and $N_{\text{max}} = 70$.

We further demonstrate the convergence of our NCSM results by applying IR extrapolation and translating the model space parameters ($N_{\text{max}}, \hbar\omega$) into an IR length scale L_{eff} and a UV scale Λ_{UV} . Selecting results obtained with a high UV cutoff $\Lambda_{\text{UV}} = 1200$ MeV—such that computations are UV converged—we perform fits to Eq. (9) with weights proportional to the inverse of the correction term (10). The extrapolation shown in Fig. 2 is performed with data up to $N_{\text{max}} = 60$, as shown by markers with a black border. The extrapolated result $E_{\infty}(\Lambda^3\text{H}) = -2.385$ MeV is presented by a red horizontal line. There is just a few keV difference between E_{varmin} at $N_{\text{max}} = 66$ and E_{∞} for this interaction which indicates a negligible many-body method uncertainty. The experimental binding energy for the hypertriton is $E_{\text{exp.}}(\Lambda^3\text{H}) = -2.35 \pm 0.05$ MeV [1].

Since we have shown that we can reach converged results (within $\sim\text{keV}$) we perform the computations with all 42 interaction models using $N_{\text{max}} = 66$ and $\hbar\omega = 9$ MeV. The resulting spread in the hypertriton

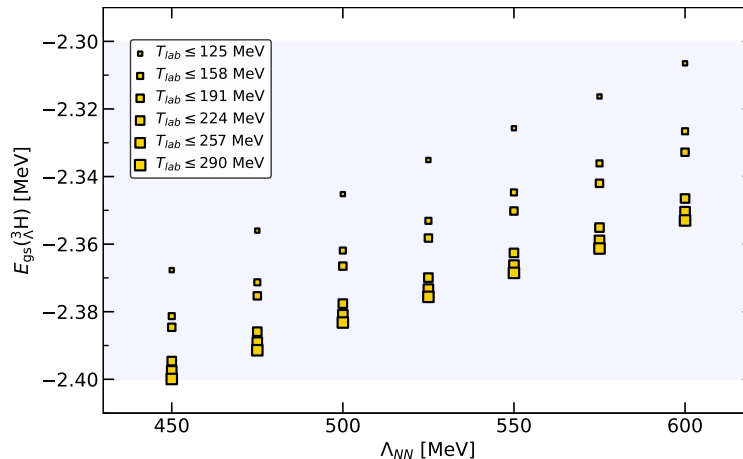


Fig. 3: The hypertriton binding energy (variational minima at $N_{\max} = 66$ and $\hbar\omega = 9$ MeV) for the 42 different NNLO_{sim} interaction models. The experimental result $E_{\text{exp.}}(\Lambda^3\text{H}) = -2.35 \pm 0.05$ MeV is represented by the blue band.

binding energy is shown in Fig. 3. The predicted binding energy decreases with increasing regulator cutoff Λ_{NN} and increases with increasing T_{Lab}^{\max} . The modest spread in the predictions indicates that the systematic uncertainty of $E(\Lambda^3\text{H})$ due to the nuclear interaction model is small. The $\lesssim 100$ keV spread of energies is basically of the same magnitude as the experimental uncertainty, while the convergence error in the many-body solver is negligible. The 100 keV spread is small compared to the wide uncertainty bands that were observed for ${}^4\text{He}$ and ${}^{16}\text{O}$ with the same family of interactions [11]. This difference can largely be attributed to the fact that the $\Lambda^3\text{H}$ system involves only two-body NN interactions while the NNN forces that are involved in ${}^4\text{He}$ and ${}^{16}\text{O}$ calculations induce much larger uncertainties. This finding of a modest systematic uncertainty opens up the opportunity to use the hypertriton binding energy as a relevant observable to constrain YN interaction models.

4 Summary and Outlook

We have estimated the uncertainty in the predicted hypertriton binding energy coming from the systematic uncertainty of the NN interaction. The small-magnitude spread ($\lesssim 100$ keV) found with the NNLO_{sim} family of interactions implies that the hypertriton binding energy provides an important constraint on YN interaction models. In the future it will be interesting to quantify uncertainties of other few- and many-body hypernuclear bound-state observables to identify additional informative constraints.

Acknowledgements The work of T.Y. Htun was supported by the Royal Golden Jubilee Ph.D. Program jointly sponsored by Thailand International Development Cooperation Agency, International Science Programme (ISP) in Sweden, and Thailand Research Fund under Contract No. PHD/0068/2558. The work of D. Gazda was supported by the Czech Science Foundation GAČR grant No. 19-19640S and by the Knut and Alice Wallenberg Foundation (PI: Jan Conrad). The work of C. Forssén was supported by the Swedish Research Council (dnr. 2017-04234). Some of the computations were performed on resources provided by the Swedish National Infrastructure for Computing (SNIC) at C3SE (Chalmers) and NSC (Linköping).

References

1. D.H. Davis, Nucl. Phys. A **754**, 3 (2005). DOI 10.1016/j.nuclphysa.2005.01.002
2. A. Nogga, Nucl. Phys. A **914**, 140 (2013). DOI 10.1016/j.nuclphysa.2013.02.053
3. D. Lonardoni, S. Gandolfi, F. Pederiva, Phys. Rev. C **87**, 041303 (2013). DOI 10.1103/PhysRevC.87.041303
4. R. Wirth, D. Gazda, P. Navrátil, A. Calci, J. Langhammer, R. Roth, Phys. Rev. Lett. **113**(19), 192502 (2014). DOI 10.1103/PhysRevLett.113.192502
5. R. Wirth, D. Gazda, P. Navrátil, R. Roth, Phys. Rev. C **97**(6), 064315 (2018). DOI 10.1103/PhysRevC.97.064315

6. L. Contessi, N. Barnea, A. Gal, *Phys. Rev. Lett.* **121**(10), 102502 (2018). DOI 10.1103/PhysRevLett.121.102502
7. H. Le, J. Haidenbauer, U.G. Meißner, A. Nogga, *Eur. Phys. J. A* **56**(12), 301 (2020). DOI 10.1140/epja/s10050-020-00314-6
8. M. Schäfer, B. Bazak, N. Barnea, J. Mareš, *Phys. Rev. C* **103**(2), 025204 (2021). DOI 10.1103/PhysRevC.103.025204
9. R.J. Furnstahl, N. Klco, D.R. Phillips, S. Wesolowski, *Phys. Rev. C* **92**(2), 024005 (2015). DOI 10.1103/PhysRevC.92.024005
10. A. Ekström, B.D. Carlsson, K.A. Wendt, C. Forssén, M.H. Jensen, R. Machleidt, S.M. Wild, *Journal of Physics G: Nuclear and Particle Physics* **42**(3), 034003 (2015). DOI 10.1088/0954-3899/42/3/034003. URL <https://doi.org/10.1088/0954-3899/42/3/034003>
11. B.D. Carlsson, A. Ekström, C. Forssén, D.F. Strömberg, G.R. Jansen, O. Lilja, M. Lindby, B.A. Mattsson, K.A. Wendt, *Phys. Rev. X* **6**(1), 011019 (2016). DOI 10.1103/PhysRevX.6.011019
12. R.N. Pérez, J.E. Amaro, E.R. Arriola, *Journal of Physics G: Nuclear and Particle Physics* **42**(3), 034013 (2015). DOI 10.1088/0954-3899/42/3/034013. URL <https://doi.org/10.1088/0954-3899/42/3/034013>
13. S. Binder, A. Calci, E. Epelbaum, R.J. Furnstahl, J. Golak, K. Hebeler, H. Kamada, H. Krebs, J. Langhammer, S. Liebig, P. Maris, U.G. Meißner, D. Minossi, A. Nogga, H. Potter, R. Roth, R. Skibiński, K. Topolnicki, J.P. Vary, H. Witala, *Phys. Rev. C* **93**, 044002 (2016). DOI 10.1103/PhysRevC.93.044002. URL <https://link.aps.org/doi/10.1103/PhysRevC.93.044002>
14. R. Navarro Pérez, J.E. Amaro, E. Ruiz Arriola, P. Maris, J.P. Vary, *Phys. Rev. C* **92**(6), 064003 (2015). DOI 10.1103/PhysRevC.92.064003
15. B. Acharya, B.D. Carlsson, A. Ekström, C. Forssén, L. Platter, *Phys. Lett. B* **760**, 584 (2016). DOI 10.1016/j.physletb.2016.07.032
16. K.A. Wendt, C. Forssén, T. Papenbrock, D. Sääf, *Phys. Rev. C* **91**(6), 061301 (2015). DOI 10.1103/PhysRevC.91.061301
17. H. Polinder, J. Haidenbauer, U.G. Meißner, *Nucl. Phys. A* **779**, 244 (2006). DOI 10.1016/j.nuclphysa.2006.09.006
18. G.P. Kamuntavicius, R.K. Kalinauskas, B.R. Barrett, S. Mickevicius, D. Germanas, *Nucl. Phys. A* **695**, 191 (2001). DOI 10.1016/S0375-9474(01)01101-0
19. R.J. Furnstahl, G. Hagen, T. Papenbrock, *Phys. Rev. C* **86**, 031301 (2012). DOI 10.1103/PhysRevC.86.031301
20. S.A. Coon, M.I. Avetian, M.K.G. Kruse, U. van Kolck, P. Maris, J.P. Vary, *Phys. Rev. C* **86**, 054002 (2012). DOI 10.1103/PhysRevC.86.054002
21. C. Forssén, B.D. Carlsson, H.T. Johansson, D. Sääf, A. Bansal, G. Hagen, T. Papenbrock, *Phys. Rev. C* **97**(3), 034328 (2018). DOI 10.1103/PhysRevC.97.034328